Risk factors of complications after thermal ablation for hepatocellular carcinoma: the role of assessment of liver background

Yuhua Xie[a,*], Jing Liu[b,*], Yifan Shi[a,c], Xiaoyan Xie[a], Jie Yu[b], Ming Xu[a], Xiaohua Xie[a], Guangliang Huang[a], Bowen Zhuang[a], Mingsen Bi[b], Dongjie Qu[b], Fangying Fan[b], Minghua Ying[b], Qingqing Sun[b], Manxia Lin[a] and Ping Liang[b]

Objective To use an elastography technology and other clinical and radiological data for assessment of liver background and analyze risk factors of complications after thermal ablation in patients with hepatocellular carcinoma.
Methods Demographics, laboratory analyses, and radiological characteristics were collected from all patients. Main elastography-related indicators included F index (fibrosis index), A index (inflammation index), ATT (attenuation coefficient), E (kPa), AREA (area of blue parts), and CORR (correlation). All complications after thermal ablation were collected. Univariate analysis was performed to detect significant variables, which subsequently entered a stepwise logistic regression analysis (conditional forward selection) to identify independent variables.
Results A total of 218 patients from October 2020 to June 2023 with 291 thermal ablation sessions were enrolled. 115 patients (52.8%) developed complications. Fifteen patients (6.9%) developed major complications. Minor complications included postoperative pain (20.6%), fever (19.3%), effusion (22.5%), and hyperammonemia (1.8%). AREA ($P = 0.034$), tumor size ($P = 0.005$), and abnormal aspartate aminotransferase (AST) ($P = 0.018$) were independent predictors for complications. F index ($P = 0.021$), tumor size ($P < 0.001$), and abnormal AST ($P = 0.047$) were independent predictors for effusion. The results of univariate analysis of infection showed that tumor size, CORR, ATT, diabetes, Child–Turcotte–Pugh grade, abnormal AST, total protein, and albumin were significant (all $P < 0.05$).
Conclusion Several radiological and combinational elastography indicators related to liver fibrosis, steatosis, or inflammation were significantly correlated with the occurrence of complications. Clinical assessment of the liver background should not be neglected in the management of postablation complications. Eur J Gastroenterol Hepatol 37: 106–113

Introduction

Hepatocellular carcinoma (HCC) is the sixth most common cancer and the fourth leading cause of cancer-related death worldwide [1]. Percutaneous thermal tumor ablation is one of the important treatments for HCC [2]. Compared with surgery, image-guided ablation is an emerging tumor treatment method, which has the advantages of minimally invasive, definite curative effect, less postoperative complications, and short hospital stay [3]. Therefore, tumor ablation therapy has an extremely important clinical position in the treatment of HCC.

Although the incidence of postablation complications is lower than that of surgery, the occurrence of various complications after ablation cannot be ignored [4]. According to the recommendation of the Society of Interventional Radiology (SIR), complications after tumor ablation could be divided into minor and major complications [5]. Complications leading to severe morbidity and disability, increased demand for more care, and hospital stay, are considered major complications, such as infection, severe bleeding, and liver failure. Other complications are considered to be minor. The side effect was considered as expected, undesired consequences that resulted in substantial morbidity, mainly including fever and postablation syndrome, fell into the category of minor complication. Some complications, such as pneumothorax, may be minor or major depending on the severity and consequences [6].

At present, most studies have focused on major complications. Studies have shown that tumor size, tumor location, and ablation method were independent predictors

European Journal of Gastroenterology & Hepatology 2025, 37:106–113

Keywords: complication, hepatocellular carcinoma, new combined elastography techniques, percutaneous thermal tumor ablation

[a]Department of Medical Ultrasonics, Sun Yat-Sen University First Affiliated Hospital, Guangzhou, Guangdong Province, [b]Department of Ultrasound, Fifth Medical Center of Chinese PLA General Hospital, Beijing and [c]Department of Ultrasound, First Affiliated Hospital of Guangzhou Medical University, Guangzhou, Guangdong Province, China

Correspondence to Ping Liang, PhD, Department of Ultrasound, Fifth Medical Center of Chinese PLA General Hospital, Beijing 100853, China
Tel: +86 01066939530; e-mail: liangping301@hotmail.com

*Yuhua Xie and Jing Liu contributed equally to the writing of this article.

Received 14 August 2024 **Accepted** 30 September 2024.

Supplemental Digital Content is available for this article. Direct URL citations appear in the printed text and are provided in the HTML and PDF versions of this article on the journal's website, www.eurojgh.com.

of major complications [7–11]. A few studies have shown that diabetes, tumor size, prior biliary intervention, and prior transarterial chemoembolization were independent predictors of infection [12–14]. However, attention to minor complications or side effects is insufficient because they do not cause serious sequelae to patients and rarely affect postoperative care. However, minor complications would still affect the quality of life and even trigger fear of cancer or treatment [15,16], thus could not be ignored.

The pathological process of liver fibrosis and cirrhosis involves the interaction of inflammation, necrosis, and fibrosis [17,18]. Patients with liver cirrhosis always have portal hypertension and hepatic insufficiency, which may affect the postoperative recovery and the occurrence of complications. Cirrhosis is also considered a systemic disease which affects many organs and systems of the body, including the immune system [19], which may be related to complications after ablation. Therefore, assessment of liver fibrosis or cirrhosis may be helpful in the evaluation of postablation complications. Nonalcoholic fatty liver disease (NAFLD) is a fatty liver disease characterized by liver metabolic syndrome. In the progressive development of liver steatosis liver cell inflammation/necrosis, it can eventually lead to cirrhosis and liver cancer. NAFLD involves several immune cell-mediated inflammatory processes. Therefore, liver steatosis is also likely to be associated with postablation complications.

Elastography, like shear wave elastography (SWE) and real-time tissue elastography (RTE), is an important noninvasive method to assess liver fibrosis. SWE, which relies on the measurement of the shear wave propagation speed in soft tissue [20], has proven to be more accurate methods for detection of liver fibrosis and cirrhosis than RTE, which is a technique for quantifying fibrosis by analyzing the characteristic data of tissue strain histogram. But diagnostic efficacy of SWE significantly varied with inflammation fluctuations [21,22]. This is also the main limitation of shear wave application in liver fibrosis. RTE is not affected by the degree of liver inflammation and only reflects the process of liver fibrosis, but it is not highly accurate for any cutoff stage of fibrosis [23,24]. Therefore, RTE and SWE complement each other, combination of the two providing a more accurate and objective assessment of liver fibrosis [25].

This study intends to use a new technology, which combined RTE and SWE, for the assessment of liver stiffness and analyze the performance of this new technology in assessing the risk of infection and minor complications after thermal ablation in patients with HCC.

Materials and methods

The protocol of this two-center study was approved by the Institutional Review Board of Chinese PLA General Hospital and the First Affiliated Hospital of Sun Yat-sen University. Informed consent was obtained from all patients after the procedures had been fully explained.

Patients

From October 2020 to June 2023, 218 patients who met the inclusion criteria and prepared to undergo thermal ablation for HCC were enrolled (Fig. 1). The diagnosis of HCC was based on the American Association for the Study of Liver Diseases (AASLD) Practice Guidance on Prevention, Diagnosis, and Treatment of Hepatocellular Carcinoma (2023 edition), and the staging of HCC was based on the Barcelona Clinic Liver Cancer (BCLC) staging (2022 edition). Combined elastography examination was performed on patients within 1 week before ablation. The patient's data and complications after ablation were retrospectively collected. Patients with unsuccessful combined elastography examination or incomplete thermal ablation were excluded.

The inclusion criteria were as follows: (1) age between 18 and 80 years; (2) patients with chronic hepatitis B virus (HBV) infection (hepatitis B surface antigen or HBV DNA were positive for more than 6 months); (3) patients with HCC within the Milan criteria (single HCC ≤ 5 cm or up to three HCCs ≤3 cm); (4) no transarterial chemoembolization was performed in the past 6 months; and (5) no systemic treatment before.

The exclusion criteria were as follows: (1) unsuccessful combined elastography examination within 1 week before ablation or unqualified elastography image and (2) incomplete thermal ablation evaluated by enhanced imaging 1 month after ablation.

Data collection

Demographics, laboratory analyses, and radiological characteristics, including upper abdominal computed tomography (CT), MRI, and ultrasound examination, were collected from all patients within 1 week before thermal ablation. The liver morphology, liver parenchyma echogenicity, portal vein diameter and flow rate, spleen size, splenic vein diameter, and flow rate were evaluated by ultrasound. The number, location, and size of lesions were evaluated by MRI or CT.

Combined elastography examination

The elastography measurement was performed within a week before ablation by one of three sonographers who have more than 200 cases of experience in elastography examination. All combined elastography data were performed using the ARIETTA 850 (Fujifilm ALOKA, Tokyo, Japan) with a convex array probe (C252, 1–6 MHz). Patient preparation includes: (1) fasting for more than 8 h; (2) rest for at least 20 min after strenuous exercise; and (3) examination in the supine position, if necessary, can choose the lateral recumbent position. Combi-Elasto mode was used to obtain data. The operator placed the probe on the right axillary midline or anterior axillary line between the ribs and perpendicular to the liver capsule. The measurement site was selected away from large vascular structures and ducts (with a diameter ≥3 mm) and at least 3 cm away from the lesions, preferably in the S5 and S8 of the liver if possible. Region of interest was placed at a depth of 1–2 cm beneath the liver capsule. Patients were asked to hold their breath for 4–5 s for examination. After the strain curve was stabilized for three cycles, press the UPDATE button to measure. After five measurements, the median was taken as the final result of the measurement. If KPa is used as the final result, interquartile range/median (IQR/M) ≤ 30% is required; if used

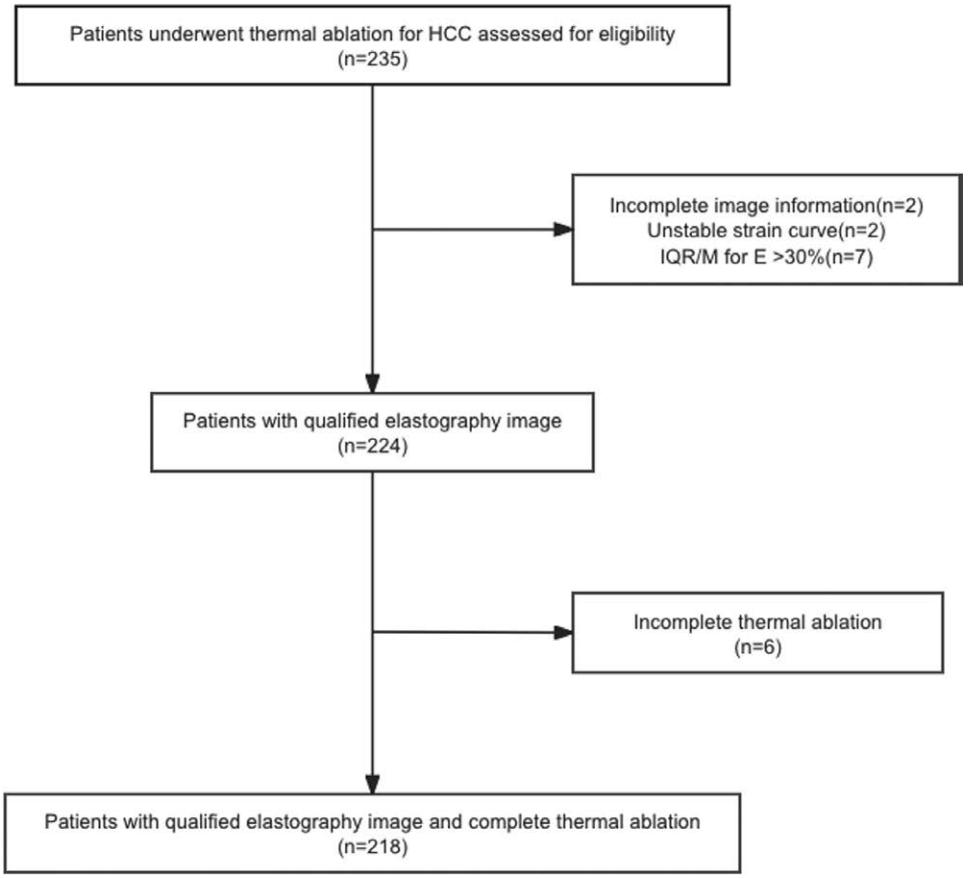

Fig. 1. Flowchart of patient selection. HCC, hepatocellular carcinoma; IQR/M, interquartile range/median.

Vs as the final result, IQR/M ≤ 15% is required. Also, shear wave VsN (Vs efficacy rate) ≥ 60% is required. The regular periodic strain curve needs to select the trough frame for analysis (Fig. 2, Supplementary Table S1, Supplemental digital content 1, *http://links.lww.com/EJGH/B84*). Combined elastography can assess the whole process of chronic liver disease. In the results, not only the F index related to the stage of liver fibrosis can be obtained, but also the A index related to the activity of inflammation can be measured at the same time. For patients with liver steatosis, the ATT (attenuation coefficient) can also be used for accurate quantitative evaluation.

Thermal ablation

Treatment strategies were decided after a multidiscipline discussion, which at least included surgeons, radiologists, oncologists, and pathologists, based on the patients' performance status, liver function, and tumor profile. Interventional radiologists with more than 10 years' of ablation experience completed the ablation of all patients. The number and placement of needles, and ablation time depended on the size and location of the tumor. For large sizes or high-risk lesions, to achieve a safe margin of 5–10 mm, a series of adjuvant measures were adopted, including multiple needle insertions and application cycles, percutaneous ethanol injection, and artificial ascites or hydrothorax.

Complications after thermal ablation

All complications within 1 month after thermal ablation were collected in this study, including major and minor complications. Two doctors with rich clinical experience judged the occurrence of postoperative complications according to the corresponding diagnostic criteria by consulting the course records, nursing records, temperature sheets, and all examination results during hospitalization. Fever is defined as body temperature ≥37.5 °C after ablation. Infection is defined as the following criteria: (1) body temperature ≥38.5 °C that was persistent for more than 3 days within 2 weeks after ablation; (2) white blood cell level >10 or <4 × 10^9/L; (3) positive culture of blood, drainage, sputum, urine, or evidence of infection found at radiologic examination [26]. Effusion is defined as newly occurred ascites or hydrothorax after ablation.

Statistical analysis

Continuous variables were compared using the Mann–Whitney *U*-test. Categorical variables were compared using the χ^2 test. Univariate analysis was performed to detect significant variables associated with complications, which subsequently entered a stepwise logistic regression analysis (conditional forward selection) to identify independent variables for complications ($P < 0.05$).

All statistical analyses were performed using SPSS (version 20.0; SPSS Inc., Chicago, Illinois, USA). All statistical

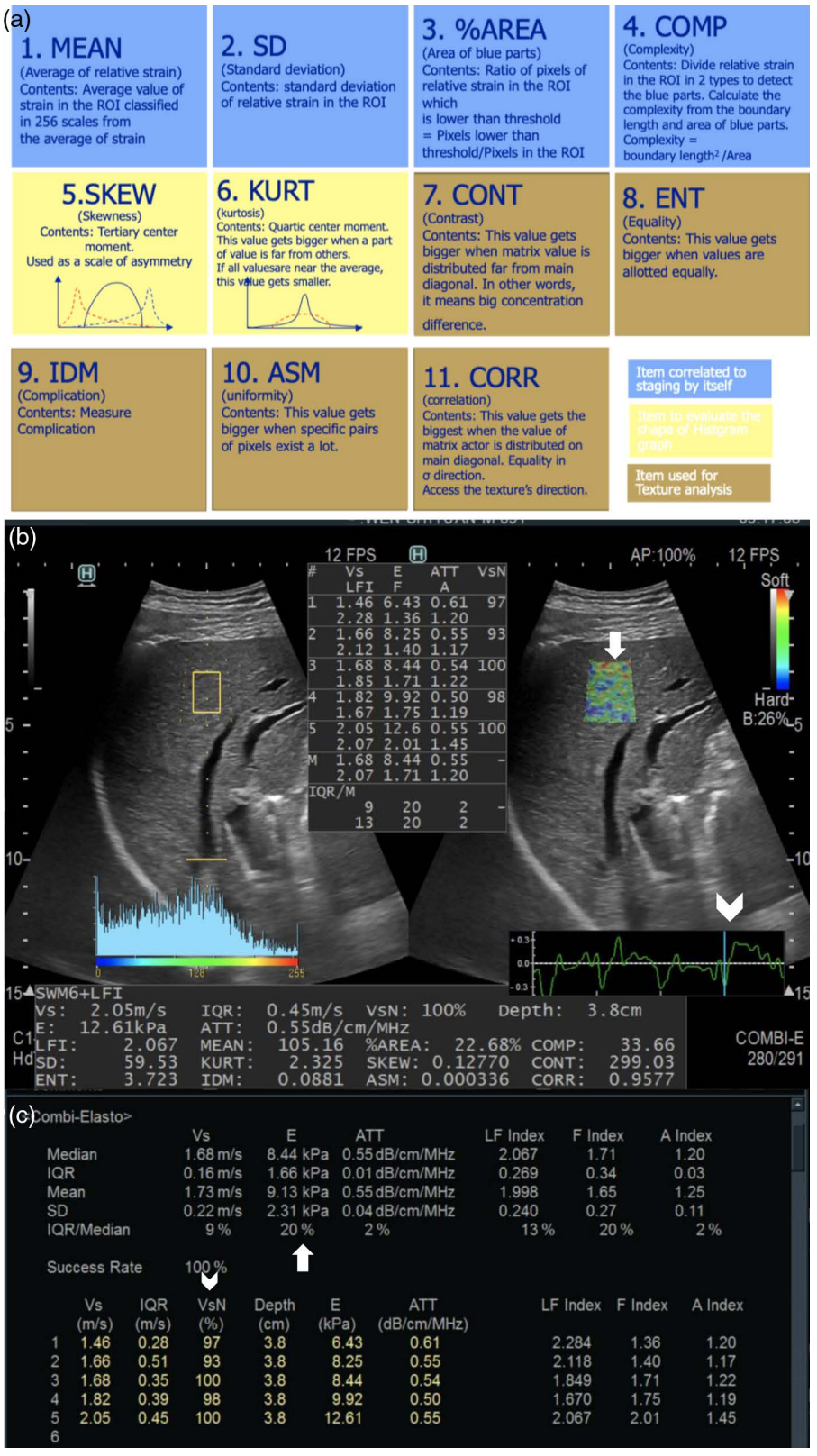

Fig. 2. Combined elastography examination. (a) Eleven items of real-time tissue elastography images. (b) The measurement site was selected away from large vascular structures and ducts (with a diameter ≥3 mm) and at least 3 cm away from the lesions, preferably in the S5 and S8 of the liver if possible. ROI (arrow) was placed at a depth of 1–2 cm beneath the liver capsule. Regular periodic strain curve needs to select the trough frame (arrowhead) for analysis. (c) Qualified image, IQR/M for E ≤ 30% (arrow) and shear wave VsN (Vs efficacy rate) ≥ 60% (arrowhead). ATT, attenuation coefficient; IQR/M, interquartile range/median; ROI, region of interest.

tests were two-tailed, and a *P*-value of less than 0.05 was considered to indicate a statistically significant difference.

Results

Patient characteristics

The baseline characteristics of the patients are summarized in Table 1. A total of 218 patients with 291 thermal ablation sessions were enrolled, comprising 182 men and 36 women, with a mean age of 56.2 ± 9.2 years. In total, 115 patients (52.8%) developed complications after percutaneous thermal ablation of their liver malignancies (Table 1). Fifteen patients (6.9%) developed major complications, including infection (5.0%), intestinal obstruction (0.9%), pneumothorax (0.5%), and arrhythmia (0.5%). Other complications were defined as minor complications, including postoperative pain (20.6%), fever (19.3%), effusion (22.5%), and hyperammonemia (1.8%).

Factors associated with overall complications

The results of univariate and multivariate analyses are shown in Table 2. According to univariate analysis, the potential factors affecting complications included international normalized ratio (INR), mean, AREA (area of blue parts), Vs, E, F index, tumor size, abnormal aspartate aminotransferase (AST), abnormal γ-glutamyl transpeptidase (GGT), and abnormal albumin (ALB) (all $P < 0.05$). Multivariate analysis showed that AREA ($P = 0.034$), tumor size ($P = 0.005$), and abnormal AST ($P = 0.018$) were independent predictors for complications.

Table 1 Patient characteristics

Index	Total (*N* = 218)	With complications (*n* = 115)	Without complications (*n* = 103)	*P*-value
Age (years)	56.2 ± 9.2	55.9 ± 9.8	56.5 ± 8.5	0.633
Male	182 (83.5%)	96 (83.5%)	86 (83.5%)	0.997
BMI (kg/m^2)	24.2 ± 3.5	23.9 ± 3.7	24.5 ± 3.1	0.168
Hypertension	36 (16.5%)	21 (18.3%)	15 (14.6%)	0.463
Diabetes	53 (24.3%)	32 (27.8%)	21 (20.4%)	0.201
ALT	23.9 (6.0–318.0)	26.0 (6.0–255.0)	22.0 (9.0–318.0)	0.096
AST	28.0 (11.1–414.0)	31.0 (11.1–362.0)	25.0 (12.0–414.0)	**0.011**
GGT	33.0 (9.0–469.0)	41.0 (9.0–469.0)	28.0 (12.0–465.0)	**0.003**
TP	64.5 (31.0–85.0)	64.2 (51.0–85.0)	65.0 (31.0–76.8)	0.555
ALB	37.7 (3.5–79.0)	37.0 (3.5–79.0)	38.0 (15.0–47.6)	0.151
TBIL	16.7 (3.2–191.0)	17.2 (3.2–191.0)	16.2 (3.3–64.0)	0.154
DBIL	5.4 (0.8–39.7)	5.8 (1.8–39.7)	4.6 (0.8–16.7)	0.079
PT	12.6 (3.0–18.9)	12.7 (3.0–18.9)	12.6 (4.1–18.2)	0.114
INR	1.1 (0.9–1.8)	1.1 (0.9–1.8)	1.1 (0.9–1.7)	**0.032**
HGB	135.5 (62.0–356.0)	135.0 (62.0–356.0)	137.0 (67.0–356.0)	0.509
PLT	133.0 (14.8–320.0)	135.0 (14.8–268.0)	129.0 (46.0–320.0)	0.959
LYMPH#	1.3 (0.1–11.6)	1.2 (0.1–11.4)	1.4 (0.3–11.6)	**0.046**
LYMPH%	30.6 (7.7–61.6)	28.9 (7.7–61.6)	32.0 (8.1–59.6)	0.142
NEUT#	2.4 (0.2–23.1)	2.3 (0.4–21.2)	2.5 (0.2–23.1)	0.571
NEUT%	56.2 (5.7–88.8)	56.4 (13.7–85.2)	55.7 (5.7–88.8)	0.825
SCr	74.0 (47.0–324.0)	72.0 (47.0–195.0)	75.3 (49.0–324.0)	0.065
Tumor size (mm)	17.0 (7.7–50.0)	19.0 (7.7–50.0)	16.0 (8.0–41.0)	**0.010**
BCLC (0/A)	108/110 (49.5%/50.5%)	56/59 (48.7%/51.3%)	52/51 (50.5%/49.5%)	0.463
High-risk location	80 (36.7%)	42 (36.5%)	38 (36.9%)	0.618
CTP grade (A/B)	154/64 (70.6%/29.4%)	81/34 (70.4%/29.6%)	73/30 (70.9%/29.1%)	0.943
MELD	6.2 (0.3–16.0)	6.5 (1.4–16.0)	6.1 (0.3–14.1)	0.795
Ablation (MWA/RFA)	181/37 (83.0%/17.0%)	99/16 (86.1%/13.9%)	82/21 (79.6%/20.4%)	0.303

Bold values indicate statistical significance if $P < 0.05$.
ALB, albumin; ALT, alanine aminotransferase; AST, aspartate aminotransferase; BCLC, Barcelona Clinic Liver Cancer; CTP, Child–Turcotte–Pugh; DBIL, direct bilirubin; GGT, γ-glutamyl transpeptidase; HGB, hemoglobin; INR, international normalized ratio; LYMPH#, lymphocyte absolute value; LYMPH%, lymphocyte percentage; NEUT#, neutrophil absolute value; NEUT%, neutrophil percentage; MELD, Model for End-stage Liver Disease; MWA, microwave ablation; PLT, platelet; PT, prothrombin time; RFA, radiofrequency ablation; SCr, serum creatinine; TBIL, total bilirubin; TP, total protein.

Table 2 Results of the univariable and multivariate analyses of complication

	Univariable analysis		Multivariate analysis	
Index	*P*-value	OR (95% CI)	*P*-value	OR (95% CI)
AST (normal/abnormal)	0.012	2.156 (1.187–3.916)	**0.018**	2.130 (1.138–3.986)
GGT (normal/abnormal)	0.005	2.367 (1.297–4.321)	0.171	1.512 (0.763–2.998)
ALB (normal/abnormal)	0.030	1.964 (1.069–3.606)	0.268	0.962 (0.453–2.044)
INR	0.032	11.274 (1.596–79.657)	0.071	4.828 (0.542–42.980)
Tumor size	0.010	1.051 (1.018–1.085)	**0.005**	1.048 (1.015–1.084)
Mean	0.017	0.972 (0.949–0.995)	0.159	0.993 (0.970–1.017)
AREA	0.016	1.028 (1.005–1.052)	**0.034**	1.026 (1.002–1.050)
Vs	0.030	1.764 (1.055–2.949)	0.137	1.290 (0.321–5.177)
E	0.018	1.050 (1.008–1.093)	0.254	1.028 (0.922–1.145)
F index	0.031	1.517 (1.040–2.214)	0.544	0.742 (0.282–1.948)

Abnormal AST: AST>37 U/L; abnormal GGT: GGT>50 U/L; abnormal ALB: ALB<35 g/L.
Bold values indicate statistical significance if $P < 0.05$.
ALB, albumin; AREA, area of blue parts; AST, aspartate aminotransferase; CI, confidence interval; F index, fibrosis index; GGT, γ-glutamyl transpeptidase; INR, international normalized ratio; mean, average of relative strain; OR, odds ratio.

Factors associated with fever

Table 3 shows the results of univariate and multivariate logistic regression of fever. According to univariate analysis, the potential factors affecting fever included age, sex, portal vein velocity, mean, abnormal prothrombin time, and abnormal neutrophil absolute value (NEUT#) (all $P < 0.05$). Multivariate analysis showed that sex ($P = 0.014$), portal vein velocity ($P = 0.021$), and abnormal NEUT# ($P = 0.008$) were independent predictors for complications.

Factors associated with pain

The results of univariate and multivariate logistic regression of pain were shown in Table 4. According to univariate analysis, the potential factors affecting pain included ALT, Vs, abnormal HBV-DNA, Child–Turcotte–Pugh (CTP) grade, abnormal total protein (TP), and high-risk location (all $P < 0.05$). Multivariate analysis showed that ALT ($P = 0.005$), abnormal HBV-DNA ($P = 0.015$), abnormal TP ($P = 0.006$), and high-risk location ($P = 0.047$) were independent predictors for pain.

Factors associated with effusion

Table 5 shows the results of univariate and multivariate logistic regression of effusion. According to univariate analysis, the potential factors affecting effusion included direct bilirubin, serum creatinine, tumor size, Vs, E, F index, abnormal HBV-DNA, abnormal AST, abnormal GGT, and abnormal total bilirubin (all $P < 0.05$). Multivariate analysis showed that F index ($P = 0.021$), tumor size ($P < 0.001$), and abnormal AST ($P = 0.047$) were independent predictors for effusion.

Factors associated with infection

The potential factors affecting infection included age, BMI, splenic vein diameter, tumor size, CORR, ATT, diabetes,

Table 3 Results of the univariable and multivariate analyses of fever

	Univariable analysis		Multivariate analysis	
Index	*P*-value	OR (95% CI)	*P*-value	OR (95% CI)
Age	0.037	0.962 (0.927–0.998)	0.109	0.967 (0.929–1.007)
Sex	0.037	0.209 (0.048–0.097)	**0.014**	0.153 (0.034–0.685)
Portal vein velocity	0.026	1.067 (1.008–1.131)	**0.021**	1.075 (1.011–1.143)
PT (normal/abnormal)	0.048	2.087 (1.008–4.322)	0.260	1.254 (0.533–2.951)
NEUT# (normal/abnormal)	0.049	1.983 (1.004–3.918)	**0.008**	2.678 (1.298–5.526)
Mean	0.017	0.967 (0.941–0.994)	0.237	0.973 (0.954–1.012)

Abnormal PT: PT>14 s; abnormal NEUT#: NEUT#<1.80 or >6.40 × 10^9/L.
Bold values indicate statistical significance if $P < 0.05$.
CI, confidence interval; mean, average of relative strain; NEUT#, neutrophil absolute value; OR, odds ratio; PT, prothrombin time.

Table 4 Results of the multivariate logistic regression of pain

	Univariable analysis		Multivariate analysis	
Index	*P*-value	OR (95% CI)	*P*-value	OR (95% CI)
ALT	0.041	1.007 (1.000–1.014)	**0.005**	1.011 (1.003–1.019)
TP (normal/abnormal)	0.012	0.394 (0.191–0.814)	**0.006**	0.338 (0.157–0.731)
HBV-DNA (normal/abnormal)	0.025	0.100 (0.013–0.754)	**0.015**	0.073 (0.009–0.572)
CTP grade	0.026	0.375 (0.158–0.891)	0.105	0.551 (0.211–1.437)
Vs	0.031	0.482 (0.248–0.935)	0.087	0.645 (0.306–1.357)
High-risk location	0.038	1.993 (1.015–3.926)	**0.047**	1.967 (1.009–3.844)

Abnormal TP: TP<64 g/L; abnormal HBV-DNA: HBV-DNA>100 IU/ml.
Bold values indicate statistical significance if $P < 0.05$.
ALT, alanine aminotransferase; CI, confidence interval; CTP, Child–Turcotte–Pugh; HBV, hepatitis B virus; OR, odds ratio; TP, total protein.

Table 5 Results of the multivariate logistic regression of effusion

	Univariable analysis		Multivariate analysis	
Index	*P*-value	OR (95% CI)	*P*-value	OR (95% CI)
AST (normal/abnormal)	0.006	2.513 (1.302–4.852)	**0.047**	2.060 (1.008–4.210)
GGT (normal/abnormal)	0.002	2.813 (1.456–5.434)	0.292	1.405 (0.637–3.102)
TBIL (normal/abnormal)	0.037	2.071 (1.043–4.112)	0.196	1.469 (0.518–4.170)
DBIL	0.008	1.094 (1.024–1.170)	0.195	1.031 (0.9320–1.142)
SCr	0.019	0.971 (0.948–0.995)	0.164	0.981 (0.967–1.007)
HBV-DNA (normal/abnormal)	0.042	2.286 (1.032–5.064)	0.360	1.835 (0.699–4.823)
Tumor size	<0.001	1.066 (1.032–1.101)	**<0.001**	1.065 (1.030–1.102)
Vs	0.029	1.945 (1.072–3.528)	0.374	0.463 (0.082–2.609)
E	0.019	1.056 (1.009–1.105)	0.443	0.979 (0.861–1.113)
F index	0.006	1.897 (1.206–2.982)	**0.021**	1.773 (1.089–2.888)

Abnormal AST: AST>37 U/L; abnormal GGT: GGT>50 U/L; abnormal TBIL: TBIL>22 μmol/L.
Bold values indicate statistical significance if $P < 0.05$.
AST, aspartate aminotransferase; CI, confidence interval; DBIL, direct bilirubin; F index, fibrosis index; GGT, γ-glutamyl transpeptidase; HBV, hepatitis B virus; OR, odds ratio; SCr, serum creatinine; TBIL, total bilirubin.

CTP grade, abnormal AST, abnormal TP, abnormal ALB, abnormal INR, and abnormal hemoglobin (HGB) (all $P < 0.05$). Because the number of infections (11 cases) is small, multivariate analysis cannot be carried out for infection.

Discussion

In this study, the incidence of and factors associated with complications were evaluated after thermal ablation treatment. Compared with other studies [9–11,14], in addition to the inclusion of laboratory results and regular imaging data, this study included the new combinational elastography analysis data in the analysis related to complications. The results of this study showed that several related indicators in combinational elastography were significantly correlated with the occurrence of different complications. The main cause of HCC in China is hepatitis B, and most chronic hepatitis can cause necrotic inflammatory activity and fibrosis [27]. Previous studies have not clearly found that liver disease is related to the occurrence of complications after ablation [9–11,14,26,28]. This study found that it is related to some complications by evaluating the degree of liver fibrosis and the degree of inflammatory activity, which provides more valuable diagnostic information for the prediction of complications after ablation and provides a new evaluation basis for the clinical management of patients after thermal ablation.

Our study found that AREA, tumor size, and abnormal AST were independent predictors of overall complications. This study showed that larger tumors lead to more complications, which is consistent with other published literature [8]. Larger tumors require longer ablation time and higher ablation energy [29]. A larger ablation area is also more likely to have a greater impact on liver function reserve. Abnormal ALT indicates that there are some problems in liver function to some extent, which can also explain why patients with abnormal ALT are more likely to have complications after ablation [30]. The AREA in combinational elastography represents the blue area, and the larger the value represents the higher degree of liver fibrosis. The results of this study showed that patients with a higher degree of liver fibrosis were more likely to have complications. Liver fibrosis represents persisting chronic liver injury and chronic inflammation, which may cause liver function damage [30].

In the analysis of the related factors of infection after ablation, a comparison between groups of patients with and without infection found that age, BMI, diabetes, AST, TP, ALB, INR, HGB, splenic vein diameter, tumor size, CTP grade, CORR, and ATT may be related to the occurrence of infection, which is also consistent with the results of previous studies [26,31,32]. Hyperglycemia in diabetic patients can cause dysfunction of immune responses, and the spread of invasive pathogens in diabetic patients cannot be controlled. Therefore, diabetic patients are more susceptible to infection [33]. Hypoalbuminemia is closely related to the occurrence and severity of infection. ALB plays an important role in antimicrobial defense and repair [34]. This study also found that ATT may be correlated with the presence of infection. The larger the proportion of adipose tissue in the liver, the higher the ultrasonic attenuation, which is the evaluation index of liver steatosis. The results of this study also showed that the degree of liver steatosis may be related to infection after ablation. Because of the low incidence of major complications after ablation, the number of infections in this study is small, multivariate analysis cannot be carried out for infection. More cases can be collected for further research.

This study also found F index was significantly correlated with the presence of effusion. In the combinational elastography technique used in this study, the F index is the fibrosis-related index. This study found that the higher the degree of liver fibrosis, the more prone to effusion after ablation, which may be related to portal hypertension in cirrhotic patients [10,14].

This study found that high-risk location may cause more pain after ablation. High-risk location was defined as the lesion within 5 mm from the important organ, blood vessel, and structure. This result suggests that if the lesion is located at a high-risk location, we need to be careful to avoid damage to important structures and take appropriate measures to protect if necessary. This study found that postoperative pain was not associated with the degree of liver fibrosis.

Because the pathological process of liver fibrosis is caused by pathogenic factors, it leads to the formation of connective tissue proliferation during the repeated repair process of liver damage caused by inflammatory reactions in liver cells [18]. So fibrosis and inflammation have always accompanied each other in the process of lesions, and the level of inflammation may predict the progression of fibrosis. ARIETTA 850 provides not only the F index but also the A index in terms of quantification, which can evaluate liver fibrosis much more accurately and completely.

The advantage of our study lies in the comprehensive collection of relevant clinical data of patients and the inclusion of a new combinational elastography technique. Our study found that the occurrence of infection and effusion in HCC patients after thermal ablation is related to the degree of liver fibrosis and the degree of liver steatosis, and reported the risk factors of each complication. A new evaluation method is proposed for patients with a high risk of complications encountered in clinical practice, which is also more conducive to guiding clinical prevention of complications after ablation. Our study pointed out that clinical assessment of the liver background should not be neglected during the management of preablation and postablation complications.

Nevertheless, our research still has some limitations. In our study, some odds ratio values are around 1. While these results were statistically significant, their clinical significance remains to be verified. We believe that the assessment of risk factors for complications should not only consider the impact of a single factor alone but also combine multiple factors, such as clinical indicators and elastography indicators, to improve the prediction of complications. Because of the limitation of the number of cases and the number of positive patients, we only figured out the risk factors of part of minor complications and infection, risk factors of other major complications remain to be further investigated. Also, this study is retrospective, we showed the indicators correlated with the occurrence of different complications. And results still need validation.

Conclusion

Our study found that several combinational elastography indicators related to liver fibrosis, liver steatosis, or inflammation were significantly correlated with the occurrence of different complications. The occurrence of complications, such as infection and effusion was related to the degree of liver fibrosis and the degree of liver steatosis. The results suggest that clinical assessment of the liver background should not be neglected in the management of preablation and postablation complications.

Acknowledgements

None.

Conflicts of interest

There are no conflicts of interest.

References

1 Sung H, Ferlay J, Siegel RL, Laversanne M, Soerjomataram I, Jemal A, *et al*. Global Cancer Statistics 2020: GLOBOCAN estimates of incidence and mortality worldwide for 36 cancers in 185 countries. *CA Cancer J Clin* 2021;71:209–249.
2 Reig M, Forner A, Rimola J, Ferrer-Fàbrega J, Burrel M, Garcia-Criado A, *et al*. BCLC strategy for prognosis prediction and treatment recommendation: the 2022 update. *J Hepatol* 2022; 76:681–693.
3 Villanueva A. Hepatocellular carcinoma. *N Engl J Med* 2019; 380:1450–1462.
4 Izzo F, Granata V, Grassi R, Fusco R, Palaia R, Delrio P, *et al*. Radiofrequency ablation and microwave ablation in liver tumors: an update. *Oncologist* 2019; 24:e990–e1005.
5 Cardella JF, Kundu S, Miller DL, Millward SF, Sacks D. Society of Interventional Radiology clinical practice guidelines. *J Vasc Interv Radiol* 2009; 20(7 Suppl):S189–S191.
6 Ahmed M, Solbiati L, Brace CL, Breen DJ, Callstrom MR, Charboneau JW, *et al*. Image-guided tumor ablation: standardization of terminology and reporting criteria – a 10-year update. *J Vasc Interv Radiol* 2014;273:241–260.
7 Huang Q, Pang M, Zeng Q, He X, Zheng R, Ge M, Li K. The frequency and risk factors of major complications after thermal ablation of liver tumours in 2084 ablation sessions. *Front Surg* 2022; 9:1010043.
8 Chen TM, Huang P-T, Lin L-F, Tung J-N. Major complications of ultrasound-guided percutaneous radiofrequency ablations for liver malignancies: single center experience. *J Gastroenterol Hepatol* 2008; 23:e445–e450.
9 Livraghi T, Meloni F, Solbiati L, Zanus G; Collaborative Italian Group using AMICA System. Complications of microwave ablation for liver tumors: results of a multicenter study. *Cardiovasc Intervent Radiol* 2012; 35:868–874.
10 Liang P, Wang Y, Yu XL, Dong B. Malignant liver tumors: treatment with percutaneous microwave ablation – complications among cohort of 1136 patients. *Radiology* 2009; 251:933–940.
11 Fonseca AZ, Santin S, Gomes LGL, Waisberg J, Ribeiro MAF. Complications of radiofrequency ablation of hepatic tumors: frequency and risk factors. *World J Hepatol* 2014; 6:107–113.
12 Kulkarni CB, Pullara SK, Rajsekar CS, Moorthy S. Complications of percutaneous radiofrequency ablation for hepatocellular carcinoma. *Acad Radiol* 2024; 31:2987–3003.
13 Li X, Zhang Y, Wang X, Zeng H, Zhou L, Huang G, *et al*. Predicting infectious complications after percutaneous thermal ablation of liver malignancies: a 12-year single-center experience. *Radiology* 2023; 308:e223091.
14 Maeda M, Saeki I, Sakaida I, Aikata H, Araki Y, Ogawa C, *et al*. complications after radiofrequency ablation for hepatocellular carcinoma: a multicenter study involving 9411 Japanese patients. *Liver Cancer* 2020; 9:50–62.
15 Wah TM, Arellano RS, Gervais DA, Saltalamacchia CA, Martino J, Halpern EF, *et al.*, Image-guided percutaneous radiofrequency ablation and incidence of post-radiofrequency ablation syndrome: prospective survey. *Radiology* 2005; 237:1097–1102.
16 Carrafiello G, Laganà D, Ianniello A, Dionigi G, Novario R, Recaldini C, *et al.*, Post-radiofrequency ablation syndrome after percutaneous radiofrequency of abdominal tumours: one centre experience and review of published works. *Australas Radiol* 2007; 51:550–554.
17 Parola M, Pinzani M. Liver fibrosis: pathophysiology, pathogenetic targets and clinical issues. *Mol Aspects Med* 2019; 65:37–55.
18 Ginès P, Krag A, Abraldes JG, Solà E, Fabrellas N, Kamath PS. Liver cirrhosis. *Lancet* 2021; 398:1359–1376.
19 Albillos A, Martin-Mateos R, Van der Merwe S, Wiest R, Jalan R, Álvarez-Mon M. Cirrhosis-associated immune dysfunction. *Nat Rev Gastroenterol Hepatol* 2022; 19:112–134.
20 Ferraioli G, Wong VW, Castera L, Berzigotti A, Sporea I, Dietrich CF, *et al*. Liver ultrasound elastography: an update to the World Federation for Ultrasound in Medicine and Biology Guidelines and Recommendations. *Ultrasound Med Biol* 2018; 44:2419–2440.
21 Zeng J, Huang Z, Jin J, Zheng J, Wu T, Zheng R. Diagnostic accuracy of 2-D shear wave elastography for the non-invasive staging of liver fibrosis in patients with elevated alanine aminotransferase levels. *Ultrasound Med Biol* 2018; 44:85–93.
22 Wu T, Wang P, Zhang T, Zheng J, Li S, Zeng J, *et al*. Comparison of two-dimensional shear wave elastography and real-time tissue elastography for assessing liver fibrosis in chronic hepatitis B. *Dig Dis* 2016; 34:640–649.
23 Paparo F, Corradi F, Cevasco L, Revelli M, Marziano A, Molini L, *et al*. Real-time elastography in the assessment of liver fibrosis: a review of qualitative and semi-quantitative methods for elastogram analysis. *Ultrasound Med Biol* 2014; 40:1923–1933.
24 Kobayashi K, Nakao H, Nishiyama T, Lin Y, Kikuchi S, Kobayashi Y, *et al*. Diagnostic accuracy of real-time tissue elastography for the staging of liver fibrosis: a meta-analysis. *Eur Radiol* 2015; 25:230–238.
25 Yazaki T, Tobita H, Sato S, Miyake T, Kataoka M, Ishihara S. Combinational elastography for assessment of liver fibrosis in patients with liver injury. *J Int Med Res* 2022; 50:3000605221100126.
26 Yin G, Zhang N, BuHe AM, Yan W, Li T, Peng J. Risk factors of secondary infection/recurrence after ablation for liver cancers: a systemic review and meta-analysis. *J Cancer Res Ther* 2022; 18:1352–1359.
27 Yao QY, Feng Y-D, Han P, Yang F, Song G-Q. Hepatic microenvironment underlies fibrosis in chronic hepatitis B patients. *World J Gastroenterol* 2020; 26:3917–3928.
28 Schullian P, Johnston E, Laimer G, Putzer D, Eberle G, Amann A, *et al*. Frequency and risk factors for major complications after stereotactic radiofrequency ablation of liver tumors in 1235 ablation sessions: a 15-year experience. *Eur Radiol* 2021; 31:3042–3052.
29 Ruiter SJS, Heerink WJ, de Jong KP. Liver microwave ablation: a systematic review of various FDA-approved systems. *Eur Radiol* 2019; 29:4026–4035.
30 Kwo PY, Cohen SM, Lim JK. ACG clinical guideline: evaluation of abnormal liver chemistries. *Am J Gastroenterol* 2017; 112:18–35.
31 Park JG, Park SY, Tak WY, Kweon YO, Jang SY, Lee YR, *et al*. Early complications after percutaneous radiofrequency ablation for hepatocellular carcinoma: an analysis of 1,843 ablations in 1,211 patients in a single centre: experience over 10 years. *Clin Radiol* 2017; 72:692.e9–692.e15.
32 Su XF, Li N, Chen X-F, Zhang L, Yan M. Incidence and risk factors for liver abscess after thermal ablation of liver neoplasm. *Hepat Mon* 2016; 16:e34588.
33 Berbudi A, Rahmadika N, Tjahjadi AI, Ruslami R. Type 2 diabetes and its impact on the immune system. *Curr Diabetes Rev* 2020; 16:442–449.
34 Wiedermann CJ. Hypoalbuminemia as surrogate and culprit of infections. *Int J Mol Sci* 2021; 22:4496.